

# Numerical Modelling of Damage Response of Layered Composite Plates

I. Smojver<sup>1</sup> and J. Sorić<sup>2</sup>

**Abstract:** The paper addresses the problem of impact on layered fibre composites. The behaviour of composite laminates under impact loading is dependent not only on the velocity but also on the mass and geometry of the impactor. Using micromechanical Mori-Tanaka approach, mechanical properties of the laminate have been calculated utilizing the material constants of the fibre and matrix. General purpose FEM software ABAQUS has been modified by means of user written subroutines for modelling of composite laminate and rigid impactor. The kinematics of the impact has been simulated using transient dynamic analysis. Employing user defined multi point constraints, delamination zones have been modeled and visualised

**keyword:** Finite element method, Layered composites, Micromechanics, Impact damage, Delaminations, Transient dynamic analysis

## 1 Introduction

Although the composite materials have been used extensively over the years, their usefulness has been impaired frequently with inability to sustain impact loading resulting in the large number of damage modes. These phenomena occur very often during the exploitation and maintenance of aerospace and ship structures, which results in the reduction of the overall stiffness and strength of the structure. This is particularly the case in tensile loaded laminates as shown by Chow and Atluri (1998). In order to simulate structural behaviour under impact loading, it is necessary to take into account large number of parameters such as mass, velocity and shape of the impactor tip as well as geometry and stiffness of the composite panel. An extensive overview of numerous computational strategies applied in the impact damage analysis of various composite structures can be found in

[Atluri (1997)]. The response of the composite structures can be generally considered as global and local. Local response is geometrically bounded to the vicinity of the impact point while global one reflects the behaviour of the whole structure. At high speed or hiperspeed impact, when the complete penetration of the laminate appears frequently, the local response is predominant due to the very short duration of the event. However, very important group of problems are those considering impact with low velocity and low mass of impactor, where the global response is predominant due to the relatively large duration of the contact [Cantwell and Morton (1989)]. It is of utmost importance to predict the appearance of various damage modes in the case of low velocity impact. One of the most dangerous are interlaminar delaminations commonly known as "Barely Visible Impact Damage" (BVID) as most of the damage in a structure remains visually undetected due to the fact that the fracture behaviour of composite structures differs significantly from that of metallic ones. This is caused by the fact that the ability of non-metallic layered composites to undergo plastic deformations is very limited, as a result of the intrinsic low ductility of the fiber and matrix. In the assessment of the appearance of damage, two terms are to be considered: damage tolerance, defined as the load carrying ability of structure after presence of damage, and damage resistance as the amount of damage appearing in the structure at particular impact case [Cantwell and Morton (1991)]. The impact itself is a progressive event, resulting in the change of material properties that has to be taken into account through the degradation of mechanical properties. In the past, most of authors have treated low-velocity impact problems as quasi-static due to the long duration of impact. The most often used, and today classical, has been the approach introduced by Sun and associates [Sun and Liou (1989)]. The history of impact forces has been reconstructed using modified Hertzian contact where exponential law is relating impact force and indentation of the laminate. This is the direct application of explicit relations developed for contact of rigid sphere and transversely isotropic

<sup>1</sup> Department of Aerospace Engineering, University of Zagreb, I. Lučića 5, HR-100000 Zagreb, Croatia; e-mail: ismojver@fsb.hr

<sup>2</sup> Department of Engineering Mechanics, University of Zagreb, I. Lučića 5, HR-100000 Zagreb, Croatia

half-plane [Willis (1966)]. Most of the numerical models apply transient dynamic analysis using very different types of elements and various models have been developed to predict the appearance of delaminations [Chang, Choi and Jeng (1990); Finn and Springer (1993); Razi and Kobayashi (1993); Collombet, Bonini and Lataillade (1996); Ganapathy and Rao (1998)]. Li and Siegmund (2004) have applied cohesive zone model approach in the analysis of delamination at interface between thin ductile film and elastic material, while Zhang and Xia (2005) analysed interphase damage by using finite element analysis on a micromechanical unit cell model. It has been experimentally proven that the appearance of slit matrix cracks in the neighbouring layers with different fibre orientation is the precursor to the appearance of interlaminar delaminations [Chang, Choi and Jeng (1990); Collombet, Bonini and Lataillade (1996)].

In this paper, the problem of delaminations in multi-layered composites has been solved in a numerically efficient way. A new computational model has been presented which can be applied on various, even very complicated structures. For numerical implementation of the new computational methodology, FEM software ABAQUS extended by means of user written subroutines has been employed. The geometry of impactor is defined using exact analytical functions which enable numerical simulation of various types of impactor tips. The calculation of contact forces has been performed by means of contact elements on the regions of impactor and laminate where the contact is to be expected. The appearance of delaminations has been modeled through multi-point constraints that have simulated the separation of initially coincident nodes, while the degradation of mechanical properties caused by the appearance of matrix cracks has been taken into account using the model introduced by Tsai [S. W. Tsai (1984); Soden, Hinton and Kaddour (1998)].

## 2 Mechanical properties of the composite

Mechanical properties of the composite are calculated using averaging stress approach [Mura (1987)] together with Eshelby's equivalent inclusion method. For the comparison between different homogenization micromechanical models, work by Yang and Becker (2004) has been consulted. Eshelby's tensor  $\mathbf{H}$  has been employed to calculate the effective material properties of composite system consisting of transversally isotropic fibre and

isotropic matrix. The equivalent inclusion method starts from the ellipsoidal inclusion whose principal axes are defined as  $a_1, a_2, a_3$  and takes into account different material properties of matrix and fiber (inclusion). Eshelby's tensor  $\mathbf{H}$  for such an inclusion gives the relation between total strain  $\epsilon_{ij}$  and strain in the inclusion  $\epsilon_{kl}^*$

$$\epsilon_{ij} = H_{ijkl} \epsilon_{kl}^*, \quad (1)$$

and is defined by the expression

$$H_{ijkl} = \frac{1}{8\pi} C_{mnlk} \int_{-1}^1 d\bar{\zeta}_3 \int_0^{2\pi} \left\{ G_{imjn}(\bar{\xi}) + G_{jmin}(\bar{\xi}) \right\} d\theta. \quad (2)$$

Herein,  $C_{mnlk}$  stands for elasticity tensor of the matrix material and  $G_{imjn}(\bar{\xi})$  is defined by the expression [Mura (1987)]

$$G_{imjn}(\bar{\xi}) = \bar{\xi}_j \bar{\xi}_n N_{im}(\bar{\xi}) / D(\bar{\xi}), \quad (3)$$

with  $D$  as determinant of  $\mathbf{K}$  matrix

$$D(\bar{\xi}) = e_{ijk} K_{i1} K_{j2} K_{k3}, \quad (4)$$

$N_{ij}$  as cofactors of matrix  $\mathbf{K}$

$$N_{ij}(\bar{\xi}) = \frac{1}{2} e_{ikl} e_{jmn} K_{km} K_{ln}, \quad (5)$$

and  $e_{ijk}$  as the permutation tensor. In the previous expressions  $\mathbf{K}$  is defined through

$$K_{ij}(\bar{\xi}) = C_{ijkl} \bar{\xi}_k \bar{\xi}_l \quad (6)$$

$$\mathbf{K}(\bar{\xi}) = \begin{bmatrix} K_{11} & K_{12} & K_{13} \\ K_{21} & K_{22} & K_{23} \\ K_{31} & K_{32} & K_{33} \end{bmatrix}. \quad (7)$$

The following transformation of variables has been employed

$$\bar{\xi}_1 = \bar{\zeta}_1 / a_1, \quad \bar{\xi}_2 = \bar{\zeta}_2 / a_2, \quad \bar{\xi}_3 = \bar{\zeta}_3 / a_3, \quad (8)$$

$$\bar{\zeta}_1 = \sqrt{1 - \bar{\zeta}_3^2} \cos \theta, \quad (9)$$

$$\bar{\zeta}_2 = \sqrt{1 - \bar{\zeta}_3^2} \sin \theta, \quad (10)$$

where  $\bar{\zeta}_i$  and  $\theta$  define the geometry of unit sphere [Mura (1987); Gavazzi and Lagoudas (1990)]. The calculation of the Eshelby's tensor has been performed by the numerical procedure formulated by Gavazzi and Lagoudas where Gauss integration is applied through the expression [Gavazzi and Lagoudas (1990)]

$$H_{ijkl} = \frac{1}{8\pi} \sum_{r=1}^M \sum_{s=1}^N C_{mnkl} \left\{ G_{imjn} \left( \theta_s, \bar{\zeta}_{3r} \right) + G_{j\min} \left( \theta_s, \bar{\zeta}_{3r} \right) \right\} w_{rs}. \quad (11)$$

Herein,  $M$  and  $N$  are the number of integration points used for integration over  $\bar{\zeta}_3$  and  $\theta$ , respectively. These parameters for numeric integration are selected depending on the geometry of generic ellipsoid characterized by values of  $a_1$ ,  $a_2$  and  $a_3$  [Mura (1987)]. For the fiber represented as cylindrical inclusion,  $a_3 \rightarrow \infty$ ,  $a_1/a_3$  is chosen to be  $10^{-40}$  while  $a_1/a_2$  equals 1.  $M$  and  $N$  are taken as 2 and 16, respectively. The mechanical properties of the composite are calculated using averaging scheme devised by Mori and Tanaka [Gavazzi and Lagoudas (1990)]

$$\mathbf{C} = \mathbf{C}_m + c_f (\mathbf{C}_f - \mathbf{C}_m) \left[ c_m \mathbf{H} \mathbf{C}_m^{-1} (\mathbf{C}_f - \mathbf{C}_m) + \mathbf{I} \right]^{-1} \quad (12)$$

$$\mathbf{S} = \mathbf{S}_m + c_f (\mathbf{S}_f - \mathbf{S}_m) \hat{\mathbf{S}} \quad (13)$$

$$\hat{\mathbf{S}} = \left[ c_m \mathbf{C}_m \mathbf{S}_f - c_m \mathbf{C}_m \mathbf{H} (\mathbf{S}_f - \mathbf{S}_m) + c_f \mathbf{I} \right]^{-1}. \quad (14)$$

In the previous expressions,  $\mathbf{I}$  is the identity matrix,  $\mathbf{C}$  and  $\mathbf{S}$  are elasticity and compliance tensor, respectively, while  $c_i$  is volume fraction of the particular constituent, with indices  $m$  and  $f$  standing for matrix and fibre, respectively. Material properties of the composite are defined in the ABAQUS user subroutine UMAT [ABAQUS (2003)], where it is necessary to define the tangential stiffness  $\mathbf{D}$

$$\mathbf{D} = \frac{\partial \Delta \sigma}{\partial \Delta \epsilon}, \quad (15)$$

with  $\Delta \sigma$  and  $\Delta \epsilon$  as stress and strain increments, respectively. Throughout the analysis, the material is assumed to be linearly elastic, therefore components of  $\mathbf{D}$  correspond to components of elasticity tensor  $\mathbf{C}$ .

### 3 Model for prediction of delaminations

Mathematical model used for contact force prediction in the case of low velocity impact has to characterise the

global movement of the structure, impactor dynamics and local deformations in the vicinity of the contact area. In contrast to the most models in the references where load is defined through the quasistatic contact forces that have to suffice the exponential contact law [Sun and Liou (1989)], in the presented model different approach was applied using the basic physical postulates that define impact conditions. Thus, the loading has been defined by applying initial conditions in the form of velocity and mass of the rigid impactor. The laminate is modeled using volume finite elements in order to accurately describe complex stress state in the impact area. The contact between impactor and laminate has been defined by means of contact elements on the surfaces of the impactor and the laminate. In order to decrease numerical cost of the computation, contact elements are defined only in the vicinity of the impact point. The kinematics of the event has been reconstructed using transient dynamic analysis [Bathe (1996)].

### 4 Basic assumptions

It is expected that delaminations are to appear on the interface of layers  $L_k$  and  $L_{k+1}$  at coincident nodes  $N_k$  and  $N_{k+1}$  (Fig. 1). The upper layer is the one that is closer to the impact point. The local material coordinate system pertinent to each layer is defined with axis 1 as the fibre direction, axis 2 in the plane of the laminate and normal to the fibre direction, and axis 3 normal to the plane of the laminate. In the formulation of the numerical model several essential assumptions have been introduced:

- matrix cracks in neighbouring layers precede delaminations;
- matrix cracks are predicted to initiate when tensile stress in the direction 2 is greater than the tensile strength of the laminate;
- delamination is to occur at the interface of layers  $L_k$  and  $L_{k+1}$  at coincident nodes  $N_k$  and  $N_{k+1}$  if there are matrix cracks in the element with node  $N_k$ , and there are at the same time matrix cracks in all elements of layer  $L_{k+1}$  having as a common node  $N_{k+1}$ ;
- after the appearance of matrix cracks some of the material properties are reduced.

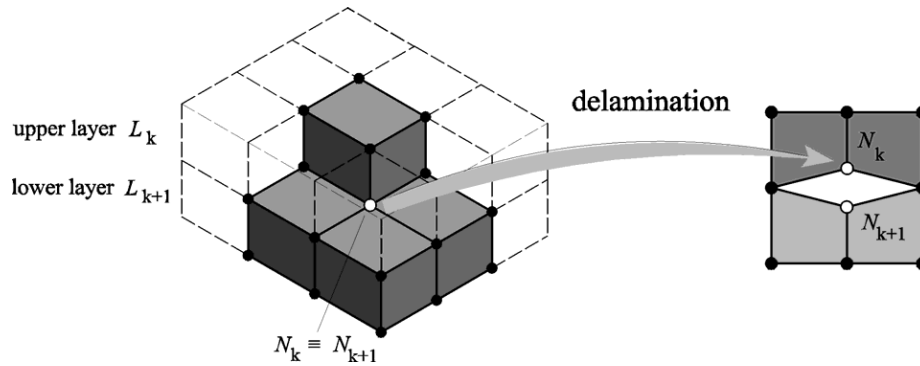


Figure 1 : The basic geometry of delaminating interface

### 5 Modeling steps

Taking into account all these assumptions, the response of the structure to the impact loading has to be modeled in several steps [Smojver (1999), Smojver, Sorić and Alfrević (2001)]:

- define the mechanical properties of the composite using the known mechanical properties of the fiber and matrix by implementing Mori-Tanaka principle in the user subroutine UMAT [ABAQUS (2003)];
- calculate the contact forces on the contact surface between impactor and laminate;
- evaluate the stress field in the laminate;
- using the user subroutine URDFIL define relations between all nodes and elements in the model in order to identify coincident nodes;
- evaluate tensile stresses in the material direction 2 and apply Hashin’s matrix failure criterion to define matrix cracks in user subroutine UMAT;
- check for the matrix cracks in the neighbouring lower layer;
- decrease corresponding values of material properties;
- define kinematic relations between coincident nodes by means of user subroutine MPC.

Hashin’s criterion for matrix cracking [Hashin (1980)], which requires the fulfilment of two conditions, has been

applied at each layer:

$$\sigma_{22} + \sigma_{33} > 0 \tag{16}$$

$$\frac{1}{Y_t^2} (\sigma_{22} + \sigma_{33})^2 + \frac{1}{S_{23}^2} (\sigma_{23}^2 + \sigma_{22} \sigma_{33}) + \frac{1}{S_{12}^2} (\sigma_{12}^2 + \sigma_{13}^2) \geq 1. \tag{17}$$

In these expressions  $\sigma_{ij}$  and  $S_{ij}$  stand for stress tensor components and corresponding shear strength values defined in material coordinate system, respectively, while  $Y_t$  is tensile stress in the direction 2. Degradation of mechanical properties in the case of the appearance of matrix cracks is defined through the expressions [Tsai (1984)]

$$E_{22} = 0.15 E_{22}^0, \nu_{12} = 0.15 \nu_{12}^0, \tag{18}$$

with  $E_{22}$  as the modulus of elasticity in direction 2 and  $\nu_{12}$  as the Poisson’s ratio for axes 1,2. Upper index ( $\dots^0$ ) stands for the material without damage.

### 6 Kinematic constraints

The initialisation of delaminations is modeled by means of user subroutine MPC (Multi Point Constraints) that enables mathematical definition of kinematic relations between coincident nodes in the computational model. The kinematic relation is generally written as

$$f_i(\mathbf{u}^1, \mathbf{u}^2, \mathbf{u}^3, \dots, \mathbf{u}^N) = 0, \quad i = 1, k, \tag{19}$$

where  $f_i$  are functions defining kinematic constraints,  $\mathbf{u}^n$  is the vector of degrees of freedom of node  $n$  that is used

```

START
  DEFINE:  relations between nodes and elements in area supposed to delaminate @ URDFIL
           nodes connected with MPCs
           mechanical properties of fibre and matrix → calculate Eshelby's tensor → calculate stiffness and
           compliance of laminate @ UMAT
           set initial conditions: mass and velocity of impactor

  BEGIN THE IMPACT: increment = 1
    calculate stress field in the plate
    FOR element Ek in Lk and node Nk
      IF (matrix fracture in element Ek → Hashin's criterion) THEN
        new degraded composite properties → Tsai @ UMAT
      TEST all neighbouring elements in layer Lk+1
        IF (matrix cracks exist in all neighbouring elements in layer Lk+1 containing node Nk) THEN
          separation of nodes Nk and Nk+1
          put new MPC between Nk and Nk+1 @ MPC
          IF (separation on all nodes on the lower side of element Ek) THEN
            delamination on the lower surface of element Ek

          new element
        IF (maximal number of increments exceeded) THEN
          END
        ELSE increment = increment + 1
    END
  END
END

```

**Figure 2** : General algorithm for calculation of matrix cracks and delaminations

in the kinematic constraints,  $N$  is number of nodes defining kinematic constraints and  $k$  is the number of dependent degrees of freedom used in the kinematic constraints [ABAQUS (2003)]. Two relations between coincident nodes are defined using the following expressions [Smjver (1999)]:

- no delamination between coincident nodes ("rigid" link)

$$f_i(\mathbf{u}^1, \mathbf{u}^2) = \mathbf{u}_i^1 - \mathbf{u}_i^2 = 0, \quad i = 1, 3, \quad (20)$$

- delamination between coincident nodes ("softened" link)

$$f_1(\mathbf{u}^1, \mathbf{u}^2) = u_1^1 - u_1^2 = 0, \quad (21)$$

$$f_2(\mathbf{u}^1, \mathbf{u}^2) = u_2^1 - u_2^2 = 0, \quad (22)$$

$$f_3(\mathbf{u}^1, \mathbf{u}^2) = k u_3^1 - u_3^2 = 0, \quad (23)$$

with  $k$  as the coefficient that determines the allowable distance between nodes after initiation of delaminations,

at the same time enabling the convergence of the solution. As may be seen from equations (19) - (22), delamination is described by the displacement component in material direction 3 at the coincident nodes.

Fig. 2. clarifies in detail steps of modeling procedure with particularly stressed ABAQUS User Subroutines applied in the analysis (in bold lettering).

## 7 Numerical examples

### 7.1 Example 1 - simply supported square plate

The impact of rigid impactor at the carbon/epoxy square plate  $[0_4/90_4]_s$  of 2 mm thickness has been investigated as the first example. The plate has dimensions  $76.2 \times 76.2$  mm and is simply supported at the edges. The impactor has hemispherical tip with radius of 3.175 mm, mass of 0.59 kg and velocity of 1.931 m/s.

Eight noded elements employing reduced integration are used in order to more accurately predict the flexural plate response. Due to the geometric and material symmetry, only one quarter of the plate has been meshed with corresponding boundary conditions applied (Fig. 3).

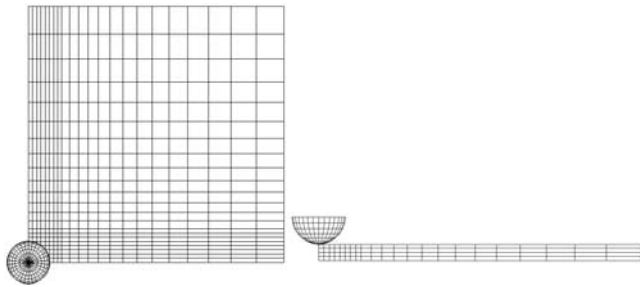


**Figure 3** : FEM model of impactor and quarter of the plate

Outer layers  $0_4$  have been modeled with one group of linear brick elements each, while the inner  $90_8$  layer has been discretised with two groups of elements in order to improve the stress calculation throughout the thickness of the plate. Total number of elements employed is 1936 [Smojver (1999), Smojver and Sori (2002)].

**Table 1** : Material properties of carbon fiber and epoxy matrix

$E_A$ [GPa]	$E_T$ [GPa]	$\nu_A$	$G_A$ [GPa]	$G_T$ [GPa]
227	15.5	0.41	23.2	5.4
$E_m$ [GPa]	$\nu_m$	$c_f$		
3.46	0.35	0.6		

**Table 2** : Strength properties of carbon/epoxy composite

$X_t$ [GPa]	$X_c$ [GPa]	$Y_t$ [MPa]	$Y_c$ [MPa]
1.5	1.5	40	246
$S_{12}$ [MPa]	$S_{23}$ [MPa]	$S_{13}$ [MPa]	
68	68	68	

The impactor has been modeled using rigid elements defined by analytical functions. The material data for transversally isotropic carbon fiber and isotropic epoxy matrix are defined in Tab. 1. In this table, index  $A$  defines the fiber direction while index  $T$  stands for the plane of transversal isotropy, with  $c_f$  as the volume fraction of the fiber in the composite. Strength properties of the composite are defined in Tab. 2 where  $X_t$  and  $X_c$  represent tensile and compressive strength in the direction 1, respectively, while  $Y_t$  and  $Y_c$  represent tensile and compressive strength in the direction 2, respectively.  $S_{ij}$  stands for shear strength properties in the main material coordinate system.

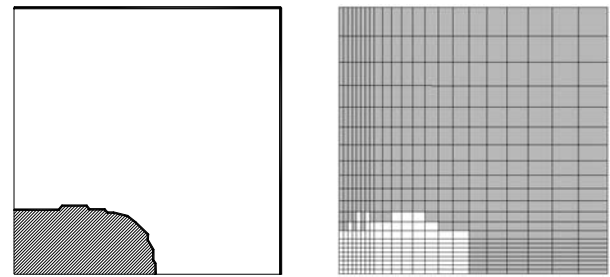


**Figure 4** : Projection of final matrix cracks in carbon/epoxy laminate  $[0_4/90_4]_s$  (left numerical values from reference [Ganapathy and Rao (1998)], right presented model)

The results of numerical research are presented in Fig. 4 and 5. Fig. 4 shows very good matching of numerically evaluated projection of matrix cracks (pale grey area) and numerical results available in [Ganapathy and Rao (1998)]. Fig. 5 shows the growth of matrix cracks in the layer the most distant from the impact point. This layer has been chosen as its behaviour is instrumental in the development of delaminations. During the impact process,  $t$  denotes the time in milliseconds measured since the first contact of impactor and the plate. As expected from the well known characteristic conical shape of matrix cracks and delaminations, the largest area of matrix cracks is recorded at the layer furthest from the impact point. The period of 1.39 ms corresponds to the downward movement of the impactor, and most of matrix cracks have developed during this part of the event. However, the final matrix cracks appeared at  $t = 2.28$  ms during the unloading part, and there are no additional cracks recorded afterwards. The impactor and plate stayed in contact for 2.8 ms [Smojver (1999)], when the bouncing of impactor begun. These results clearly indicate the growth of matrix cracks in the laminate even during the unloading phase of the process.

## 7.2 Example 2 - clamped circular plate

As the second example, the impact of rigid impactor on the  $[0_3/90_4/0_3]$  glass/epoxy composite circular plate is numerically simulated. The plate is clamped along the edges and its geometry is defined by diameter of 160 mm and thickness of 1.9 mm. The impactor has mass of 2.3 kg and results for two impactor's velocities, 2.9 and 5 m/s, have been presented.

Using material and geometric symmetry as in the pre-

[0<sub>4</sub>/90<sub>8</sub>/0<sub>4</sub>] - 1.1 J - layer 4 (0<sub>4</sub>)

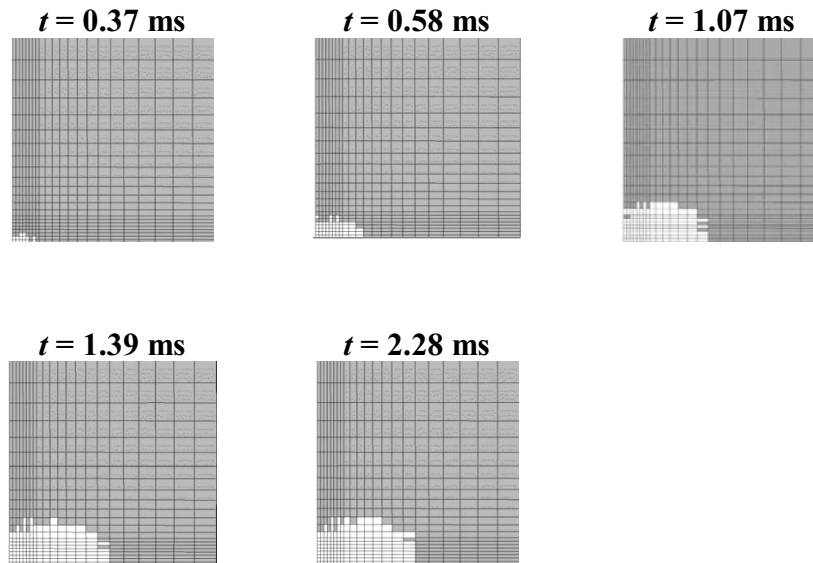


**Figure 5 :** Development of matrix cracks in the layer 4 of laminate [0<sub>4</sub>/90<sub>8</sub>/0<sub>4</sub>] due to the impact of impactor with mass of 0.59 kg and velocity of 1.931 m/s

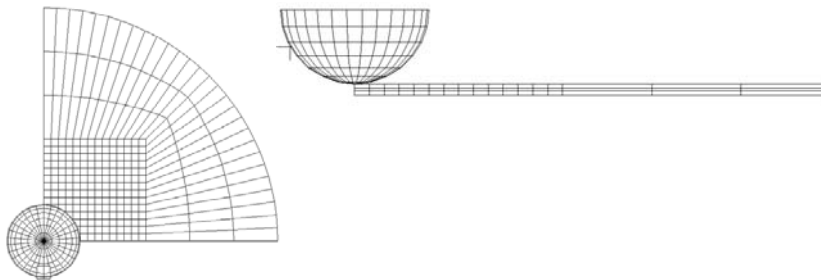


**Figure 6 :** FEM model of impactor and quarter of the plate

vious example, a quarter of the plate was modelled by 840 8-noded elements ranged in three groups [Smojver (1999)] as shown in Fig. 6. The impactor with hemispherical tip of 12.5 mm radius was modeled in the fashion similar to the Example 1.

The material data for transversally isotropic glass fiber and isotropic epoxy matrix are defined in Tab. 3 and 4, with notation having the same meaning as in the previous example.

Fig. 7 illustrates the deformed configuration of the plate during the loading and unloading phase of the impact. The loading phase takes 4.1 ms [Smojver (1999)] while at  $t = 8.0$  ms bouncing of the impactor occurs as the result of the elasticity of the plate. As obvious from Fig. 7, the bending behavior of the plate is very pronounced. Fig. 8

**Table 3 :** Material properties of glass fiber and epoxy matrix

$E_A$ [GPa]	$E_T$ [GPa]	$\nu_A$	$G_A$ [GPa]	$G_T$ [GPa]
220	14	0.2	34	5.5
$E_m$ [Gpa]		$\nu_m$	$c_f$	
3.46		0.35	0.6	

**Table 4 :** Strength properties of glass/epoxy composite

$X_t$ [GPa]	$X_c$ [GPa]	$Y_t$ [MPa]	$Y_c$ [MPa]
1.062	0.61	40	118
$S_{12}$ [MPa]		$S_{23}$ [MPa]	$S_{13}$ [MPa]
72		72	72

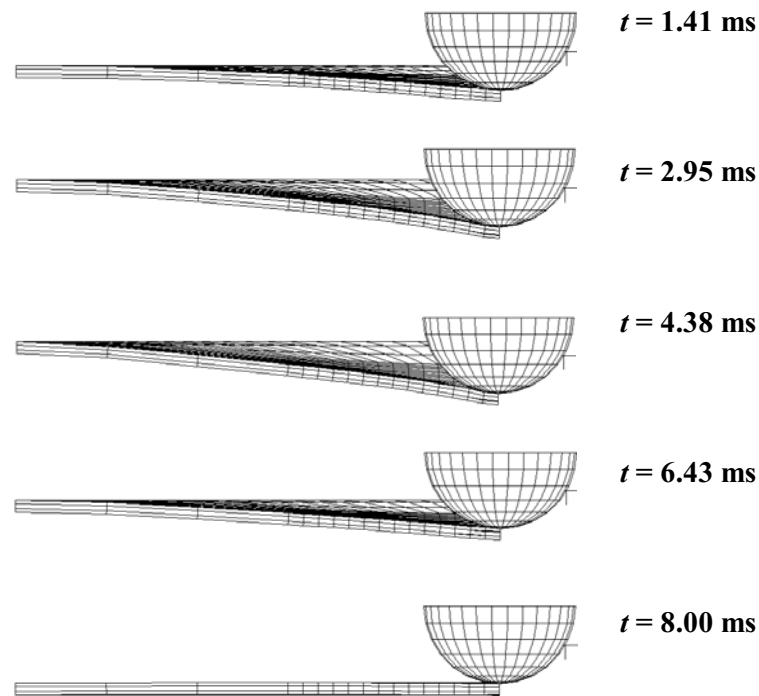


**Figure 7 :** The response of the glass/epoxy laminate  $[0_3/90_4/0_3]$  to the impact of the impactor with mass of 2.3 kg and velocity of 2.9 m/s

illustrates the comparison of matrix cracks obtained using C-scan [Bonnini (1995)] and numerical model. Only the central part of the plate is displayed because the damage is expected in this area. The region of total matrix cracks indicated using these methods is comparable, although there are differences in the shape of damage areas.

The matching is excellent in the central layer of the plate, while there is significant discrepancy between these methods in the layer furthest from the impact point. However, even in this case both methods display comparable total damage area. The delamination areas determined by present computation are compared with results of experimental investigation in Fig. 9. There is large similarity, although it is obvious that numerical procedure is more conservative, indicating larger delamination areas than recorded experimentally. As expected, the largest delamination area is recorded at the interface furthest from the impact point. Development of delaminations has been shown at Fig. 10. Although the bouncing of impactor starts at  $t = 3.03$  ms, it is obvious that delaminations grow during the unloading phase up till the last recorded value at  $t = 3.47$  ms.

## 8 Conclusions

The numerical model that predicts the appearance of matrix cracks and interlaminar delaminations induced by the low velocity impact has been presented. The model is numerically efficient and applicable to various laminate geometries and material layups. The loading is modeled using rigid analytical elements enabling various types of impactors and impactor tips to be applied in the future research. Usage of general purpose software ABAQUS gave the possibility of efficiently using various types of elements in order to more accurately describe the real structures. By applying ABAQUS User Subroutines in the defining of mechanical properties, the capabilities of the software are greatly improved. In addition, user defined subroutines enabled visualisation of areas of matrix cracks and delaminations. The developed numerical model enables monitoring of damage growth during the loading and unloading phase of the impact. It is clearly visible that damage appears in both periods, although the largest portion of final damage area is initiated before unloading begins. As expected, the largest damage areas appear in the layers that are the most distant from the impact point. The presented numerical model could be used in the assessment of low velocity impact damage in other

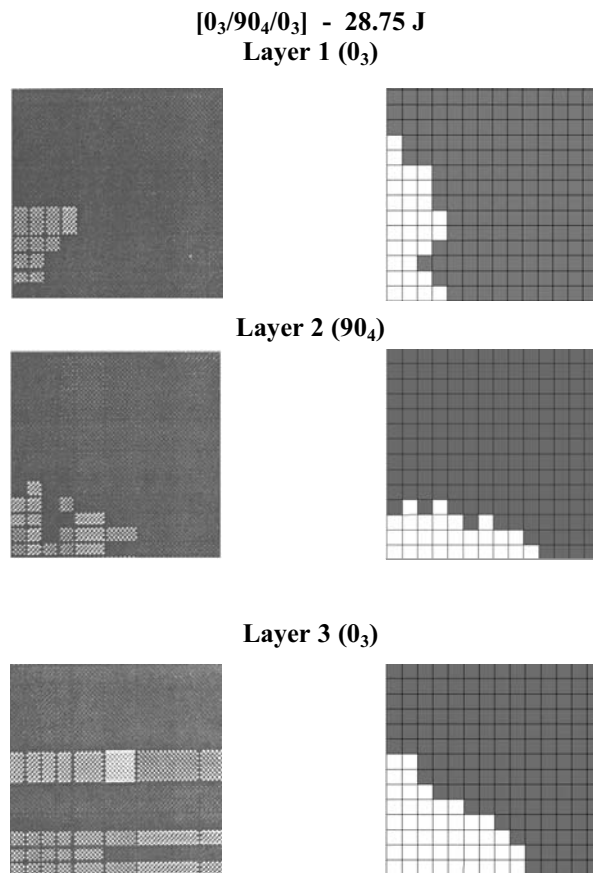


**Figure 8** : Matrix cracks in the carbon/epoxy laminate [0<sub>3</sub>/90<sub>4</sub>/0<sub>3</sub>] due to the impact of impactor with mass of 2.3 kg and velocity of 5 m/s (left experimental values by [Bonnini (1995)], right presented model)

types of shell-like structures, what is the next stage of the research.

**Acknowledgement:** The authors would like to express their gratitude to the Alexander von Humboldt Foundation for donating the computational equipment used in this research. In addition, the authors wish to thank Prof. D. C. Lagoudas for kindly providing the subroutines that have been used as the basis for calculation of mechanical properties of the composite.

## References

- ABAQUS Inc.** (2003): *ABAQUS/Standard v 6.4 User's Manual*
- Atluri, S.N** (1997): *Structural Integrity & Durability*, Tech Science Press, Forsyth.

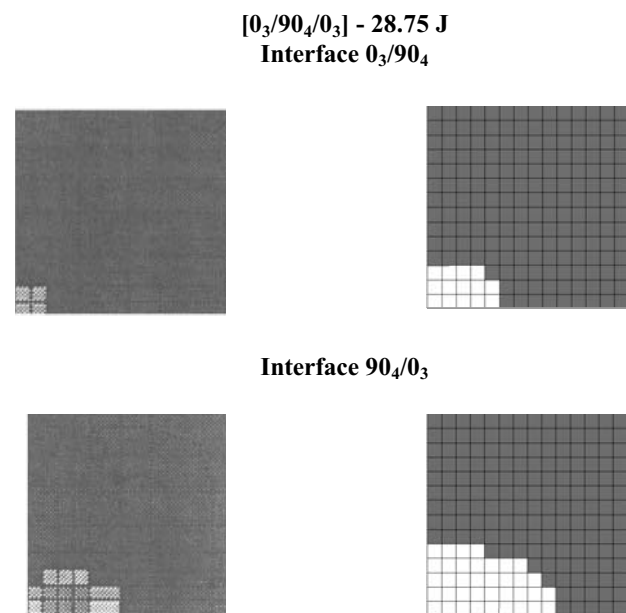


**Figure 9** : Delaminations in the carbon/epoxy laminate [0<sub>3</sub>/90<sub>4</sub>/0<sub>3</sub>] due to the impact of impactor with mass of 2.3 kg and velocity of 5 m/s (left experimental values by [Bonnini (1995)], right presented model)

**Bathe, K. J.** (1996): *Finite Element Procedures*, Prentice Hall, New Jersey.

**Bonnini, J.** (1995): *Contribution a la prediction numerique de l'endommagement de stratifies composites sous impact basse vitesse*. Dissertation, Ecole Nationale Superieure d'Arts et Metiers Centre de Bordeaux, Bordeaux.

**Cantwell, W. J.; Morton, J.** (1989): Comparison of the low and high velocity impact response of CFRP. *Composites*, vol. 20, pp. 545-551.

**Cantwell, W. J.; Morton, J.** (1991): The impact resistance of composite materials - a review. *Composites*, vol. 22, pp. 347-362.

**Chang, F. - K.; Choi, H. Y.; Jeng, S.-T.** (1990): Study of impact damage in laminated composites. *Mech. Mat.*, vol. 10, pp. 83-95.

**Chow, W. T.; Atluri, S. N.** (1998): Stress intensity factors as the fracture parameters for delamination crack growth in composite laminates, *Comp. Mech.*, vol. 21, pp. 1 - 10.

**Collombet, F.; Bonini, J.; Lataillade, J. L.** (1996): *A three-dimensional modelling of low velocity impact*

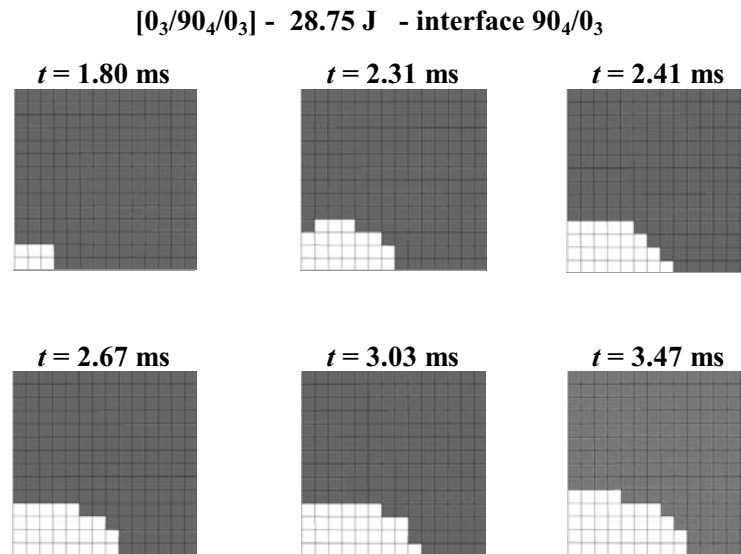


**Figure 10** : Development of delaminations at the interface 90<sub>4</sub>/0<sub>3</sub> of the laminate [0<sub>3</sub>/90<sub>4</sub>/0<sub>3</sub>] due to the impact of impactor with mass of 2.3 kg and velocity of 5 m/s

damage in composite laminates. *Int. J. Num. Meth. Eng.*, vol. 39, pp. 1491-1516.

**Finn, S. R.; Springer, G. S.** (1993): Delaminations in composite plates under transverse static or impact loads - A model. *Comp. Struct.*, vol. 23, pp. 177-190.

**Ganapathy, S.; Rao, K. P.** (1998): Failure analysis of laminated composite cylindrical / spherical shell panels subjected to low velocity impact. *Comput. Struct.*, vol. 68, pp. 627-641.

**Gavazzi, A. C.; Lagoudas, D. C.** (1990): On the numerical evaluation of Eshelby's tensor and its application to elastoplastic fibrous composites. *Comp. Mech.*, vol 7, pp. 13-19.

**Hashin, Z.** (1980): Failure criteria for unidirectional fiber composites, *J. Appl. Mech.*, vol. 47, pp. 329 – 334.

**Li, W.; Siegmund, T.** (2004): Numerical Study of Indentation Delamination of Strongly Bonded Films by Use of a Cohesive Zone Model. *CMES: Computer Modeling in Engineering & Sciences*, vol. 5, no. 1, pp. 81-90.

**Mura, T.** (1987): *Micromechanics of Defects in Solids*, Martinus Nijhoff, Dordrecht.

**Razi, H.; Kobayashi, A. S.** (1993): Delamination in cross-ply laminated composite subjected to low-velocity impact. *AIAA Journal*, vol. 31, pp. 1408-1502.

**Smojver, I.** (1999): Delamination of Multilayered Com-

posites Due to Transversal Impact Loading (in Croatian with abstract in English). Dissertation, University of Zagreb, Faculty of Mechanical Engineering and Naval Architecture, Zagreb.

**Smojver, I.; Sorić, J.; Alfirević, I.** (2001): Computational prediction of matrix cracks and delaminations in layered composites, Proceedings of the 2<sup>nd</sup> European Conference on Computational Mechanics, Z. Waszczyn, E. Stein (eds.), Cracow, CD-ROM

**Smojver, I.; Sorić, J.** (2002): Impact damage analysis of layered composite plates, Proceedings of the 7<sup>th</sup> International Design Conference - Design, Cavtat, 1255 – 1260.

**Soden, P. D.; Hinton, M. J.; Kaddour, A. S.** (1998): A comparison of the predictive capabilities of current failure theories for composite laminates. *Composite Sci. Tech.*, vol. 58, pp. 1225-1254.

**Sun, C. T.; Liou, W. J.** (1989): Investigation of laminated composite plates under impact dynamic loading using a three-dimensional hybrid stress finite element method. *Comput. Struct.*, vol. 33, pp. 879 – 884.

**Tsai, S. W.** (1984): A survey of macroscopic failure criteria for composite materials. *J. Reinf. Plast. Comp.*, vol. 3, pp. 40-62.

**Yang, Q.-S.; Becker, W.** (2004): A Comparative Investigation of Different Homogenization Methods for Prediction of the Macroscopic Properties of Composites.

*CMES: Computer Modeling in Engineering & Sciences*,  
vol. 6, no. 4, pp. 319-332.

**Willis, J. R.** (1966): Hertzian Contact of Anisotropic  
Bodies. *J. Mech. Phys. Sol.*, vol.14, pp. 163-176.

**Zhang, Y; Xia, Z.** (2005): Micromechanical Analysis  
of Interphase Damage for Fiber Reinforced Composite  
Laminates. *CMC: Computers, Materials, & Continua*,  
vol. 2, no. 3, pp. 213-226.

